Structural and photoluminescence properties of terbium-doped zinc oxide nanoparticles

Ningthoujam Surajkumar Singh[a)b)], Shougaijam Dorendrajit Singh[a)†], and Sanoujam Dhiren Meetei[a)]

[a)] *Department of Physics, Manipur University, Canchipur, Imphal* 795003, *Manipur, India*
[b)] *Department of Physics, Pachhunga University College, College Veng, Aizawl* 796001, *Mizoram, India*

(Received 2 October 2013; revised manuscript received 28 October 2013; published online 25 March 2014)

We present in this paper a study of the structural and photoluminescence (PL) properties of terbium (Tb) doped zinc oxide (ZnO) nanoparticles synthesized by a simple low temperature chemical precipitation method, using zinc acetate and terbium nitrate in an isopropanol medium with diethanolamine (DEA) as the capping agent at 60 °C. The as-prepared samples were heat treated and the PL of the annealed samples were studied. The prepared nanoparticles were characterized with X-ray diffraction (XRD). The XRD patterns show the pattern of typical ZnO nanoparticles and correspond with the standard XRD pattern given by JCPDS card No. 36-1451, showing the hexagonal phase structure. The PL intensity was enhanced due to Tb^{3+} doping, and it decreased at higher concentrations of Tb^{3+} doping after reaching a certain optimum concentration. The PL spectra of Tb^{3+} doped samples exhibited blue, bluish green, and green emissions at 460 nm ($^5D_3$ – $^7F_3$), 484 nm ($^5D_4$ – $^7F_6$), and 530 nm ($^5D_4$ – $^7F_5$), respectively, which were more intense than the emissions for the undoped ZnO sample. Based on the results, an energy level schematic diagram was proposed to explain the possible electron transition processes.

Keywords: zinc oxide, nanoparticles, photoluminescence, chemical precipitation

PACS: 81.07.Bc, 78.55.Et **DOI:** 10.1088/1674-1056/23/5/058104

1. Introduction

Owing to a direct wide band gap (3.37 eV), a large exciton binding energy (60 meV), and superior conducting properties based on oxygen vacancies, wurtzite-structured zinc oxide (ZnO) has become one of the most promising materials for the fabrication of optoelectronic devices operating in the blue and ultraviolet (UV) region and transparent conducting and piezoelectric materials that can be used to fabricate solar cells, electrodes, and sensors.[1–6] During the last few years, ZnO has been synthesized and used as the cathode material for field emission.[7–9] Consequently, ZnO nanostructures have been studied extensively owing to their potential applications in nano-devices and optical materials.[10–15] In order to design the electrical, optical, and magnetic properties of ZnO for practical applications, control of the shape and crystal structure is very important, and the synthesis of novel nanostructures is highly desired.[1] However, it has been realized that tuning the band gap only by changing the morphology or size of nanocrystals is not well suited for some applications, such as fluorescent imaging and nano-electronics.[16,17] Doping ZnO with selective elements has become an important route for enhancing and controlling its optical, electrical, and magnetic performance, which is usually crucial for their practical applications.[1] Rare earth (RE) ions incorporated into ZnO nanoparticles result in remarkable changes in the optical properties of ZnO.[10,18] Of the many RE ions, Tb^{3+} ion is an important dopant element for the green emission band.[10,19] ZnO:Tb^{3+} nanoparticles are assumed to be a new type of green phosphor with interesting photoluminescence (PL) properties.[1,19] In this work, the ZnO:Tb^{3+} nanoparticles were synthesized by a very low temperature chemical precipitation method in an isopropanol medium with diethanolamine (DEA) as the capping agent. This method has many advantages in terms of cost, minimal facilities, and energy consumption. The ZnO:Tb^{3+} nanoparticles showed PL emissions related to the intra 4f transitions of Tb^{3+} ions. The structural and PL properties of ZnO:Tb^{3+} nanoparticles have been discussed in detail.

2. Experiment

The synthesis of ZnO:Tb^{3+} nanoparticles was performed using a low temperature chemical precipitation method modified from the procedure reported by Zhou *et al*.[20] For a typical preparation, 0.3 ml of DEA was added to 100 ml isopropanol taken on a beaker and stirred well using a magnetic stirrer. We then added required amounts of zinc acetate and terbium nitrate to the above solution to obtained desired percentages of doping concentrations of terbium on ZnO. The reactants were kept stirring and the pH value of the mixture was adjusted between 9 and 10. Heat was then applied and the temperature was raised to 60 °C and maintained at that temperature for 40 min. The clear solution obtained was then allowed to cool and was kept at room temperature. The precipitation formed in 7 to 10 days. The precipitates (Ppt) that

†Corresponding author. E-mail: dorendrajit@yahoo.co.in

© 2014 Chinese Physical Society and IOP Publishing Ltd

were formed were collected by centrifugation and washed with excess methanol and dried at 100 °C. The collected samples were finally heat treated by annealing at 500 °C for 1 h, and so undoped ZnO and ZnO:Tb^{3+} nanoparticles with different Tb^{3+} concentrations of doping were synthesized. The compositions of the synthesized nanoparticles were quantified by energy-dispersive analysis of X-ray (EDAX) using the energy-dispersive X-ray (EDX) spectrometer attached to a scanning electron microscope (SEM), FEI Quanta 250. The samples were characterized for crystal phase identification by powder X-ray diffraction (XRD) using an X'Pert PANalytical X-Ray diffractometer with Cu K_α radiation. The morphology and particle size of the samples were examined with transmission electron microscopy (TEM) by using JEOL JEM-2100. For TEM measurements, a few droplets of powder, ultrasonically dispersed in alcohol, have been placed on standard carbon coated copper grids. PL measurements were taken on a LS 55 PerkinElmer fluorescence spectrophotometer with a xenon lamp as the excitation source at room temperature.

3. Results and discussion

EDAX measurements were performed to confirm the presence of Tb^{3+} in the synthesized ZnO:Tb^{3+} nanoparticles and to determine their compositions, which was also performed for the undoped ZnO nanoparticles. Figure 1 shows the EDAX spectra of the undoped ZnO and the Tb^{3+} doped ZnO samples. Figure 1(a) gives the EDAX spectrum of the undoped ZnO, showing that the nanoparticles are composed of Zn and O. The EDAX results reveal that the prepared Tb^{3+} doped nanoparticles are assuredly composed of Tb, Zn, and O. The Tb^{3+} concentrations of the prepared nanoparticles are found to be 0.52 at.%, 1.25 at.%, 1.51 at.%, and 3.40 at%, respectively, in Figs. 1(b)–1(e), depending on the Tb/Zn precursor ratio. In general, less Tb is found than provided in the precursor solution, which indicates the hindering of the dopant incorporation into the host lattice. This may happen because of the difficulties associated with the doping of RE ions into the ZnO host. Firstly, the ionic radii of RE ions (e.g., $Tb^{3+} \sim 0.92$ Å) are much larger than that of the Zn^{2+} ion (~ 0.74 Å); and secondly, the substitution creates a charge imbalance, as RE^{3+} ions (charge: +3) substitute the Zn^{2+} sites (charge: +2) in the ZnO host matrix. The charge compensation from the local defect sites results in a lattice deformation, which is not desired.[21] Henceforth, the samples will be denoted by the atomic percentage of Tb^{3+} concentrations; that is, 0 (for undoped ZnO), 0.52, 1.25, 1.51, and 3.40, as obtained in the EDAX measurements. Figure 2 shows the XRD patterns of the prepared samples with different dopant concentrations of Tb^{3+} annealed at 500 °C for 1 h. From the XRD patterns shown in Fig. 2, it can be clearly seen that the characteristic diffraction peaks of ZnO

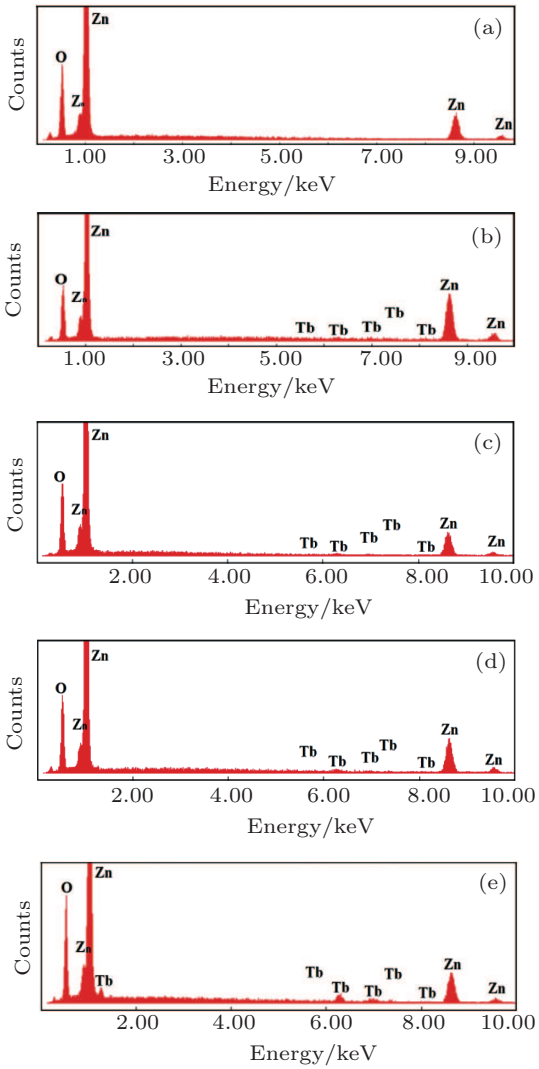


Fig. 1. (color online) EDAX spectra of ZnO:Tb^{3+} for (a) undoped, (b) 0.52 at.%, (c) 1.25 at.%, (d) 1.51 at.%, and (e) 3.4 at.% of Tb^{3+} doping concentrations.

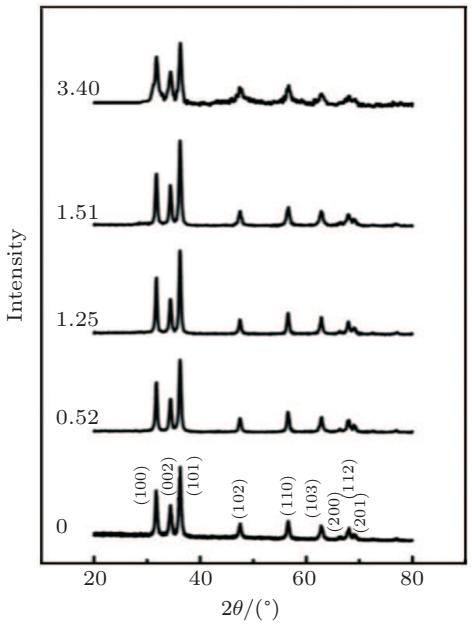


Fig. 2. XRD spectra of undoped and Tb^{3+} doped ZnO at different doping concentrations.

appear as in the standard JCPDS file for ZnO (Card No. 36-1451, $a = b = 3.249$ Å and $c = 5.206$ Å) and can be indexed to the hexagonal wurtzite structure of ZnO.[22] The sizes of the nanoparticles are calculated by Debye–Scherrer's equation[22]

$$D = \frac{0.9\lambda}{B\cos\theta}, \tag{1}$$

where D is the crystallite size, λ is the wavelength of radiation (X-ray) used, θ is the Bragg angle, and B is the full width at half maxima (FWHM). The crystallite sizes of the nanoparticles were found to be 15.4 nm for the undoped ZnO and 17.4 nm, 18.8 nm, 16.7 nm, and 14 nm for ZnO:Tb^{3+} nanoparticles with Tb^{3+} doping concentrations of 0.52 at.%, 1.25 at.%, 1.51 at.%, and 3.40 at.%, respectively.

Transmission electron microscopy (TEM) and high-resolution transmission electron microscopy (HRTEM) observations of the samples were carried out. TEM images showing the morphologies and the size distributions of the samples are shown in Fig. 3.

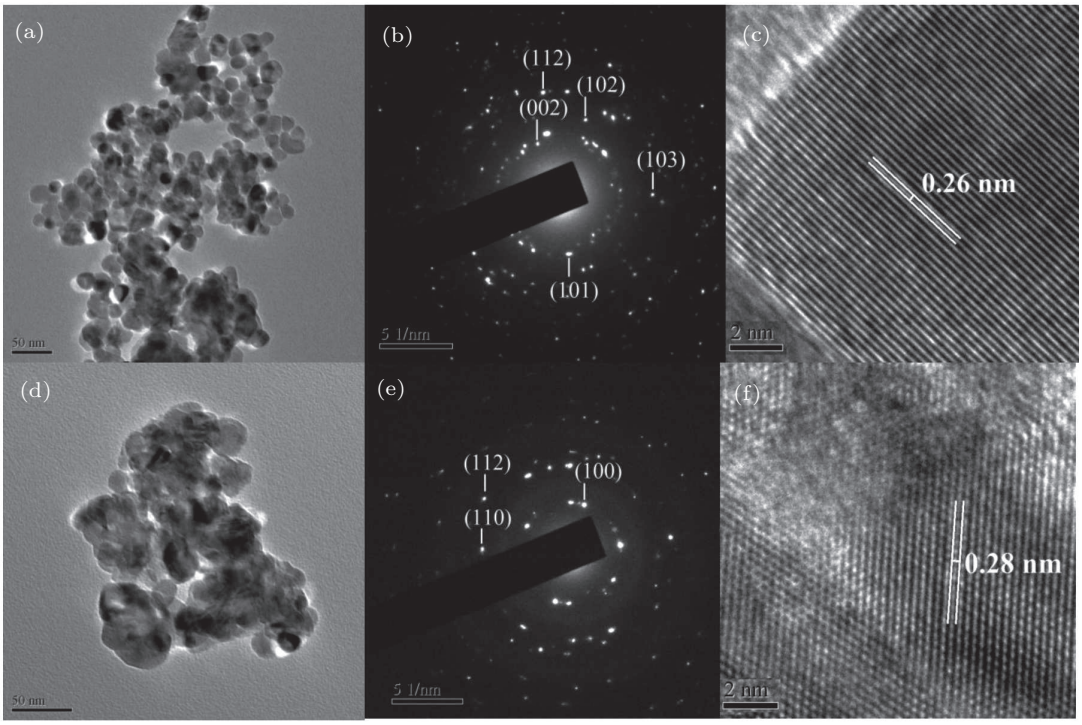


Fig. 3. (a) TEM micrograph, (b) SAED pattern, (c) HRTEM image for undoped ZnO and (d) TEM micrograph, (e) SAED pattern, (f) HRTEM image for 1.51 at.% Tb^{3+} doped ZnO.

A sample of the undoped ZnO with uniform and well-distributed spherical particles having average diameters in the range from 12 nm to 25 nm is shown in Fig. 3(a). This is consistent with the estimated value (15.4 nm) from XRD peak broadening. The selected area electron diffraction (SAED) is shown in Fig. 3(b) for the undoped ZnO nanoparticles, indicating the highly crystalline nature of the sample. Diffraction spots corresponding to the (002), (101), (102), (103), and (112) lattice planes are identified. An HRTEM image is shown in Fig. 3(c). The lattice spacing in Fig. 3(c) is found to be 0.26 nm, corresponding to the (002) plane for the undoped sample, which is in agreement with the standard values of wurtzite ZnO. Figure 3(d) shows the TEM image of the 1.51 at.% Tb^{3+} doped sample with a size range from 16 nm to 32 nm, which is consistent with the value (16.7 nm) calculated from XRD. SAED for the 1.51 at.% Tb^{3+} doped sample is shown in Fig. 3(b). Diffraction spots corresponding to the (100), (110), and (112) lattice planes are identified here. The lattice constants calculated from the SAED pattern corresponding to the identified lattice planes are in good agreement with the standard data. An HRTEM image for the 1.51 at.% Tb doped ZnO sample is shown in Fig. 3(f). The lattice spacing is estimated to be 0.28 nm, corresponding to the (100) plane, which is in agreement with the standard values of wurtzite ZnO in JCPDS Card No. 36-1451.

PL properties of the nanoparticles were recorded at room temperature to study both the excitation and the emission spectra. Figure 4 shows the emission spectra of the undoped ZnO nanoparticles taken in the emission range from 350 nm to 600 nm when excited at 240 nm. The PL emission is very well fitted with five Gaussian peaks. It is seen from the figure that the PL spectrum can be decomposed into five Gaussian components, whose peaks are located at 389 nm, 404 nm, 435 nm, 483 nm, and another broadband centered at 496 nm. The fluorescence at 389 nm corresponds to the characteristic band edge emission.[23] The violet luminescence (404 nm) has

been assigned to the electronic transition to the energy level for oxygen interstitial (O_i), which is 0.4 eV above the top of the valence band.[24]

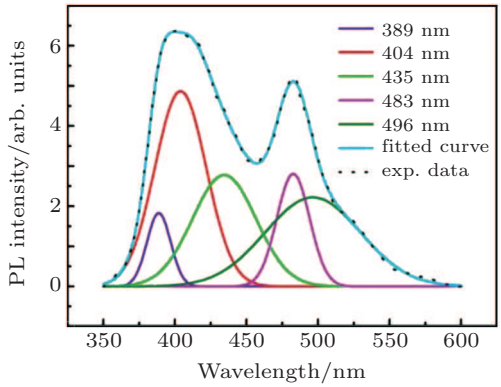


Fig. 4. (color online) PL emission spectrum of undoped ZnO with decomposed Gaussian components.

The violet luminescence (435 nm) observed in the present case has been assigned to the electronic transitions from the zinc interstitial (Zn_i) level to the valence band.[23] The energy level for neutral oxygen vacancy V_O is 2.57 eV above the valence band and is, therefore, responsible for the emission at 483 nm.[22,25,26] The broadband emission centered at 496 nm arises from the recombination of electron–hole pairs trapped at shallow and deep surface states formed by oxygen vacancy V_O and other defects.[27,28]

Figure 5 shows the excitation spectra of the ZnO:Tb^{3+} samples with different percentages of Tb doping concentrations taken in the excitation range from 200 nm to 400 nm by monitoring the emission at 485 nm. Four peaks are observed at 240 nm, 255 nm, 285 nm, and 344 nm. While the peaks up to 300 nm are due to the f–d transitions, the peaks starting from 300 nm are due to the f–f transitions of the Tb^{3+} ions.[29] The wavelengths of these peaks were used as the excitation wavelengths for further study of the emission spectra.

Figure 6(a) shows the emission spectra of ZnO:Tb^{3+} nanoparticles with different percentages of Tb doping concentrations taken in the wavelength range of 350 nm to 700 nm excited at 240 nm. Figures 6(b)–6(d) show the emission spectra excited at 255 nm, 285 nm, and 344 nm, respectively.

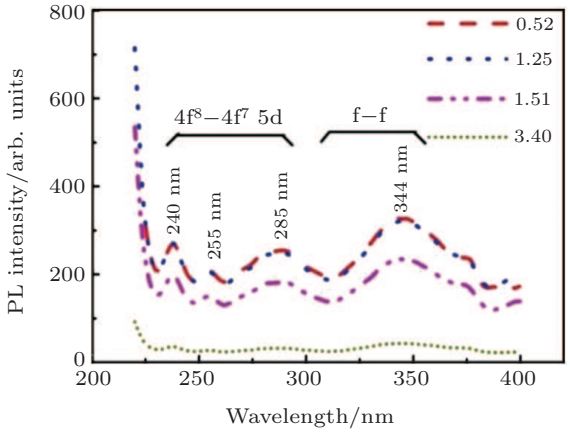


Fig. 5. (color online) PL excitation spectra of Tb^{3+} doped ZnO nanoparticles.

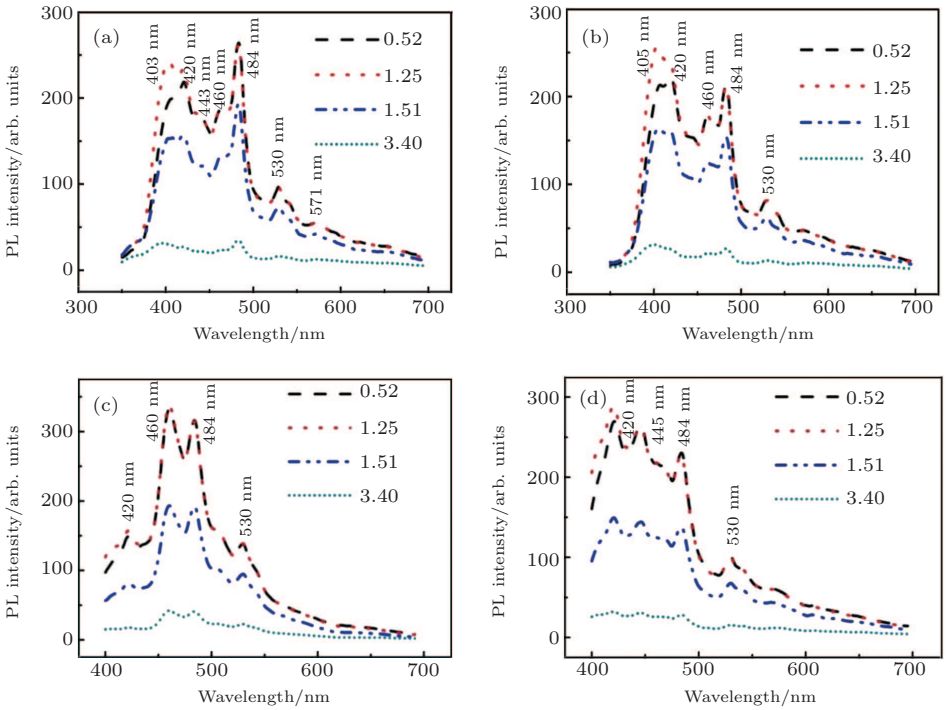


Fig. 6. (color online) PL emission spectra with different doping concentrations taken in the emission range from 350 nm to 700 nm, with excitation wavelengths (a) 240 nm, (b) 255 nm, and from 400 nm to 700 nm with excitation wavelengths (c) 285 nm, (d) 344 nm.

The doped samples show emission peaks centered at 405 nm, 420 nm, 445 nm, 484 nm, and 530 nm for all Tb concentrations. The peak intensity for the doped samples increases up to 1.25 at.% of Tb^{3+}; beyond that, it decreases as the concentration of doping increases. This may be due to the concentration quenching of the Tb^{3+} ions. Consequently, the optimum dopant concentration is found to be 1.25 at.% in this study. It is also observed that the intensity of emission at the violet end of the spectrum decreases as the excitation wavelength increases. The peaks at 405 nm, 420 nm, and 445 nm are attributed to different defects associated with the host lattice. The bluish green and green emission peaks at 460 nm, 484 nm, and 530 nm arise from Tb^{3+} 4f–4f transitions.[10,27,30,31]

Figure 7 presents a schematic drawing for possible electron transitions to illustrate the mechanism of the excitation and emission process according to the results in this work. When the ZnO:Tb^{3+} nanoparticles are excited by the 240 nm line of an Xe lamp, an electronic transition occurs from the valence band (VB) to an exciton band.[10] And then, a series of nonradiative processes occur, which are denoted by the dotted lines in the figure. Then, the electrons are trapped at the surface states of the particles, and the consequent recombination from the surface states to VB results in a broadband emission. These excited carriers are also trapped at Tb^{3+} centers, which leads to the characteristic emission peaks of Tb^{3+}, and are denoted by solid lines in the diagram.[27] The emission at 460 nm originates from Tb^{3+} 4f–4f transition $^5D_3$ – $^7F_3$.[30] The emissions at 484 nm and 530 nm are assigned to $^5D_4$ – $^7F_6$[21,32] and $^5D_4$ – $^7F_5$, respectively.[10] The emission at 490 nm is also assigned to $^5D_4$ – $^7F_6$ of Tb^{3+}.[33] The other peaks at 405 nm, 420 nm, and 445 nm probably originate from defect states, such as Zn and oxygen interstitials and oxygen vacancies.[24,34,35]

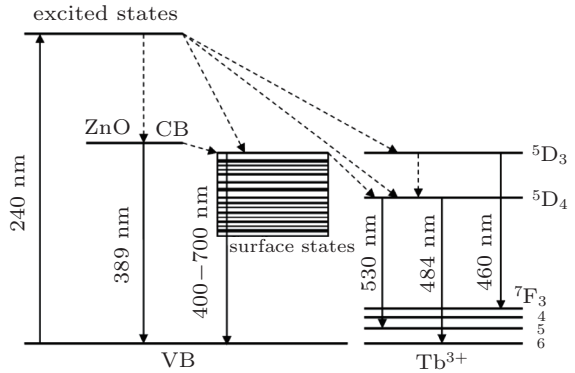


Fig. 7. Schematic drawing for possible electron transitions to illustrate the mechanism of excitation and emission process.

4. Conclusion

In conclusion, ZnO:Tb^{3+} nanoparticles with various Tb contents were prepared. XRD spectra demonstrated the substitution of Tb^{3+} ions to the Zn^{2+} sites in the ZnO wurtzite structure. Emissions from both Tb^{3+} ions and intrinsic defect states of ZnO were observed in PL studies. There was a quenching of the emission intensity as the doping concentration increased, and in this study the optimum dopant concentration was found to be 1.25 at.%. The Tb^{3+} ions have an important effect on the UV emission of ZnO. In addition, the characteristic emissions of Tb^{3+} ions were observed. For all of the samples, the carrier relaxation from the excited states of ZnO hosts to dopant result in the characteristic emission of Tb^{3+} ions.

References

[1] Li G, Lu X, Su C and Tong Y 2008 *J. Phys. Chem. C* **112** 2927
[2] Huang M H, Mao S, Feick H, Yan H, Wu Y, Kind H, Weber E, Russo R and Yang P 2001 *Science* **292** 1897
[3] Pan Z W, Dai Z R and Wang Z L 2001 *Science* **291** 1947
[4] Xu L, Su Y, Chen Y, Xiao H, Zhu L, Zhou Q and Li S 2005 *J. Phys. Chem. B* **109** 5491
[5] Rau U and Schmidt N 2001 *Thin Solid Films* **387** 141
[6] Dwivedi C and Dutta V 2012 *Adv. Nat. Sci.: Nanosci. Nanotechnol.* **3** 015011
[7] Wang J C 2013 *Chin. Phys. B* **22** 068504
[8] Wang X P, Wang Z, Wang L J and Mei C Y 2011 *Chin. Phys. B* **20** 105203
[9] Gong J F, Dou Z M, Wang Z Q, Zhang B, Zhu W H, Zhang K X, Liu M Y, Zhu H and Zhou J F 2012 *Chin. Phys. B* **21** 068101
[10] Zhao S, Wang L, Yang L and Wang Z 2010 *Physica B* **405** 3200
[11] Yang L, Tang Y H, Hu A P, Chen X H, Liang K and Zhang L D 2008 *Physica B* **403** 2230
[12] Leiter F, Alves H, Pfisterer D, Romanov N G, Hofmann D M and Meyer B K 2003 *Physica B* **340–342** 201
[13] Jokela S J, McClumskey M D and Lynn K G 2003 *Physica B* **340–342** 221
[14] Bai X D, Wang E G, Gao P X and Wang Z L 2003 *Nano Lett.* **3** 1147
[15] Ganesan P G, McGuire K, Kim H, Gothard N, Mohan S, Rao A M and Ramanath G 2005 *J. Nanosci. Nanotechnol.* **5** 1125
[16] Bailey R E and Nie S 2003 *J. Am. Chem. Soc.* **125** 7100
[17] Wang Y S, Thomas P J and O'Brien P 2006 *J. Phys. Chem. B* **110** 21412
[18] Sernelius B E, Berggren K F, Jin Z C, Hamber I and Granqvist C G 2008 *Phys. Rev. B* **37** 10244
[19] Lin J, Huang Y, Zhang J, Gao J, Ding X, Huang Z and Tang C 2007 *Chem. Mater.* **19** 2585
[20] Zhou H, Yi D, Yu Z, Xiao L and Li J 2007 *Thin Solid Films* **515** 6909
[21] Pal P P and Manam J 2013 *Nanosystems: Phys. Chem. Math.* **4** 395
[22] Sharma P K, Dutta R K and Pande A C 2010 *J. Coll. Int. Sc.* **345** 149
[23] Mishra A K, Chaudhuri S K, Mukherjee S, Priyam A, Saha A and Das D 2007 *J. Appl. Phys.* **102** 103514
[24] Devi S K L and Sudarsanakumar K 2010 *J. Lumin.* **130** 1221
[25] Chakrabarti S, Ganguli D and Chaudhuri S 2003 *J. Phys. D: Appl. Phys.* **36** 146
[26] Zhou H, Alves H, Hofman D M, Kriegsens W, Meyer B K, Kaezmarezyk G and Hoffmann A 2002 *Appl. Phys. Lett.* **80** 210.
[27] Liu S M, Liu F Q, Guo H Q, Zhang Z H and Wang Z G 2000 *Phys. Lett. A* **271** 128
[28] Mo C M, Li Y H, Liu Y S, Zhang Y and Zhang L D 1998 *J. Appl. Phys.* **83** 4389
[29] Pal P P and Manam J 2013 *Materials Sci. Eng. B* **178** 400
[30] Lin H Y, Cheng C L, Lin Y S, Hung Y, Mou C Y and Chen Y F 2011 *Nanoscale Research Lett.* **6** 503
[31] Panigrahi B S 1999 *J. Lumin.* **82** 121
[32] Dincer O and Ege A 2013 *J. Lumin.* **138** 174
[33] Huong T T, Anh T K, Khuyen H T, Hien P T and Minh L Q 2012 *Adv. Nat. Sci.: Nanosci. Nanotechnol.* **3** 015010
[34] Goswami N and Sharma D K 2010 *Physica E* **42** 1675
[35] Djurisic A B, Ng A M C and Chen X Y 2010 *Progress in Quantum Electronics* **34** 191